

Structural Identifiability of Impedance Spectroscopy Fractional-Order Equivalent Circuit Models With Two Constant Phase Elements

Tohid Soleymani Aghdam, Seyed Mohammad Mahdi Alavi, Mehrdad Saif

Abstract—Structural identifiability analysis of fractional-order equivalent circuit models (FO-ECMs), obtained through electrochemical impedance spectroscopy (EIS) is still a challenging problem. No peer-reviewed analytical or numerical proof does exist showing that whether impedance spectroscopy FO-ECMs are structurally identifiable or not, regardless of practical issues such as measurement noises and the selection of excitation signals. By using the coefficient mapping technique, this paper proposes novel computationally-efficient algebraic equations for the numerical structural identifiability analysis of a widely used FO-ECM with Grünwald-Letnikov fractional derivative approximation and two constant phase elements (CPEs) including the Warburg term. The proposed numerical structural identifiability analysis method is applied to an example from batteries, and the results are discussed. Matlab codes are available on github.

Index Terms—Structural identifiability, numerical methods, fractional order models, electrochemical impedance spectroscopy, energy storage systems, biomedical systems.

I. INTRODUCTION

Electrochemical impedance spectroscopy (EIS) is an important tool for the study of dynamics and properties of biomedical and electrochemical energy storage systems. EIS is used in [1]–[6] to study the *in vitro* and *in vivo* properties of electrode-tissue in neural stimulation techniques. In [7] and [8], EIS is used for differentiating between normal and malignant prostate tissues. Cancer detection by using EIS is studied in [9]–[17]. EIS has widely been used for monitoring of electrochemical energy storage systems in renewable energies and electric transportation. With EIS, electrochemical behaviors of batteries, super-capacitors and fuel-cells are estimated. It is shown that many specifications such as state of charge, age, internal temperature and resistance, and in general, state of health of electrochemical energy storage systems are identifiable by using EIS [18]–[33].

In EIS, an excitation signal is applied to the system, and its response is measured. If excitation signal is current, the voltage

response is collected or vice versa. The current and voltage signals are then employed for the computation of impedance spectra. The EIS data is further analyzed by fitting to an equivalent circuit model (ECM), [34] and references therein.

Figure 1 shows a typical EIS impedance spectra and its fractional-order ECM (FO-EM) that is the focus of this paper, and widely used in both biomedical and energy applications [1]–[3], [12]–[22]. The intersection of the impedance spectra and the real axis represents the high-frequency ohmic resistance R_∞ . The mid-frequency semi-circle, modeled by a parallel R_1 and $1/(C_1s^{\alpha_1})$, and the low-frequency line, modeled by $1/(C_2s^{\alpha_2})$, represent charge transfer resistance, double layer capacitance, and diffusion processes, where s is the Laplace operator and α_i 's, $i = 1, 2$, are fractional exponents between 0 and 1, ($1 > \alpha > 0$). The term $1/C_i s^{\alpha_i}$ is referred to as the constant phase element (CPE), as its phase is constant with respect to frequency. The dimension of C_i , $i = 1, 2$ is $\text{Fcm}^{-2} s^{\alpha_i-1}$ [29]. The low frequency impedance $1/(C_2 s^{\alpha_2})$ is the so-called Warburg term.

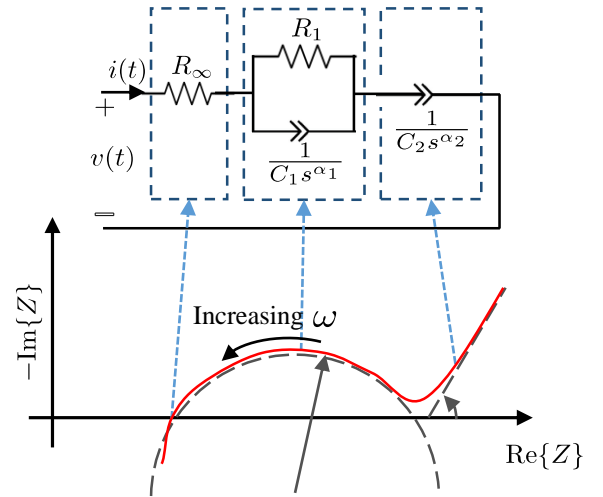


Fig. 1: The widely used fractional-order equivalent circuit model (FO-ECM) with two constant phase elements (CPEs) including the Warburg term, and corresponding impedance spectra.

Estimation of the EIS FO-ECMs has been the topic of many papers. Usually, EIS impedance spectra is firstly computed and plotted in the Nyquist diagram by using Fourier transforms,

T. Soleymani Aghdam is with the Faculty of Electrical Engineering, Shahid Beheshti University, Daneshjou Boulevard, Tehran, Iran, Postal Code 1983969411. Email: t_soleymani@sbu.ac.ir

S. M. M. Alavi is with the Department of Applied Computing and Engineering, School of Technologies, Cardiff Metropolitan University, Llandaff Campus, Western Avenue, Cardiff, UK, CF5 2YB. Email: malavi@cardiffmet.ac.uk

M. Saif is with the Department of Electrical Engineering, University of Windsor, Windsor, ON, Canada, N9B 3P4. Email: msai@uwindsor.ca

M. Saif acknowledges the research funding from the Natural Sciences and Engineering Research Council of Canada (NSERC).

Matlab codes are available online at:
<https://github.com/smmalavi/str-identifiability-frac-sys>

Corresponding Author: S. M. M. Alavi

and ECM parameters are then estimated by fitting to the impedance spectra in the frequency domain, [18], [19], [28]. An alternative approach estimates ECM parameters directly from the time-domain current and voltage signals by using system identification methods without Fourier transforms, [22], [29], [34], [35]. Estimation of the FO-ECM's parameters is beyond the scope of this paper, and interested readers are directed to [36]–[39] for a more comprehensive survey of the proposed parameter estimation techniques.

The first essential stage in parameter estimation or system identification problems is to show that the model is structurally identifiable, regardless of practical issues such as measurement noises and the selection of excitation signals and parameter estimation method, [40]–[42].

Since the 1970's, several analytical techniques have been proposed for structural identifiability analysis by using Taylor series expansion [45], [46], similarity transformations [47]–[53], differential algebra [54], [55], and Laplace transforms (transfer functions) [56], [57]. However, almost all of the proposed techniques deal with ordinary differential equations with integer orders.

This paper studies structural identifiability of the FO-ECM in Fig. 1, with two CPEs under Grünwald-Letnikov derivative approximation, which is widely employed in the literature, [6], [21], [22], [30]–[32]. In the arXiv preprint [59], the structural identifiability of the single-CPE FO-ECM is addressed by using the coefficient mapping technique. It is graphically proved that there is a one-to-one map between the coefficients of the transfer function and the parameters, and thus, the single-CPE FO-ECM is globally identifiable. It is further shown in [59] that the structural identifiability of the two-CPE FO-ECM depends on the solution of the following set of equations:

$$\begin{aligned} g_1 + g_0(T+1) \left(\frac{1}{\alpha_1 - T} + \frac{1}{\alpha_2 - T} \right) &= 0 \\ g_2 - g_0(T+1)(\hat{a} + \hat{b} + \hat{c}) &= 0, \end{aligned} \quad (1)$$

where g_i 's, $i = 0, 1, 2$ are the lowest orders' coefficients of the ECM transfer function, T is the total number of samples taken from the voltage and current signals, and

$$\begin{aligned} \hat{a} &= \frac{T}{(\alpha_2 - T)(\alpha_2 - T + 1)}, \quad \hat{b} = \frac{(T+1)}{(\alpha_1 - T)(\alpha_2 - T)} \\ \hat{c} &= \frac{T}{(\alpha_1 - T)(\alpha_1 - T + 1)}. \end{aligned}$$

However, these equations suffer from an ill-conditioned problem that is: for large T 's, g_i 's tend to zero. Under the ill-conditioned problem, it is hard to solve (1), and deduce the structural identifiability.

A. The main contribution of this paper

The main contribution of this paper is to propose alternative set of equations which do not face with the ill-conditioned problem. The new equations are computationally more efficient, compared to those in [59], and their numerical solution determines whether the two-CPE FO-CEM is structurally identifiable or not. The proposed numerical structural identifiability

analysis method is applied to the battery EIS FO-ECMs and the results are discussed.

B. Assumptions

The following assumptions are made throughout this paper.

- Due to complexities, this paper only addresses the two-CPE FO-ECMs with Grünwald-Letnikov fractional derivative approximation. Structural identifiability analysis for higher-order FO-ECMs and/or by using other approximations of fractional derivatives remains an open problem.
- This paper only focuses on the structural identifiability analysis, dealing with the model structure under the noise-free condition. The practical identifiability analysis, i.e., the selection of the excitation signals and parameter estimation technique, and the effect of measurement noise are beyond the scope of this paper. In [58], practical identifiability of fractional commensurate-order models is studied, where all differential orders are integer multiples of a base order. The proposed analysis is in the frequency domain, showing that fractional commensurate-order models are poorly identifiable for small values of the base order, [58]. In [22], practical identifiability of the single-CPE and two-CPE FO-ECMs are studied, and the results confirm that the input signal plays a key role in the parameter estimation. The selection of the excitation signal for the identification of FO-ECMs is still an open problem. In [34], [35], [43], [44], a number of methods are proposed for the selection of the excitation signal for the identification of the ordinary-order ECMs.

C. The structure of the paper

This paper is organized as follow. Section II describes FO-ECMs using the Grünwald-Letnikov approximation. In section III, the proposed structural identifiability analysis method is described. Numerical results are given and studied in section IV for an example from battery applications.

II. MODEL STRUCTURE

By using the Grünwald-Letnikov approximation, a transfer function of the FO-ECM in Fig. 1 is given by, [22], [59]:

$$H(z, \theta) = d(\theta) + \sum_{i=1}^2 \frac{b_i(\theta)z^T}{z^{T+1} - \sum_{j=0}^T a_{i,j}(\theta)z^{T-j}} \quad (2)$$

where, z is the discrete-time operator, i denotes the i -th CPE, j denotes the j -th sample, T is the total number of samples, and

$$\begin{aligned} \theta &= \{R_\infty, R_1, C_1, \alpha_1, C_2, \alpha_2\}, \quad d(\theta) = R_\infty, \\ b_i(\theta) &= \frac{T_s^{\alpha_i}}{C_i}, \quad a_{1,0}(\theta) = \alpha_1 - \frac{T_s^{\alpha_1}}{R_1 C_1}, \\ a_{2,0}(\theta) &= \alpha_2, \quad a_{i,j}(\theta) = -(-1)^{j+1} \binom{\alpha_i}{j+1}, \\ i &= 1, 2, \quad j = 1, 2, \dots, T, \end{aligned} \quad (3)$$

where, $\binom{\alpha_i}{j}$ is the binomial coefficient given by

$$\binom{\alpha_i}{j} = \frac{\Gamma(\alpha_i + 1)}{\Gamma(j + 1)\Gamma(\alpha_i + 1 - j)},$$

and, $\Gamma(\cdot)$ denotes the gamma function.

By the expansion of (2), a monic transfer function, where the coefficient of the highest order term in the denominator is 1, is given by, [22], [59]:

$$H(z, \theta) = \frac{f_{2T+2}(\theta)z^{2T+2} + f_{2T+1}(\theta)z^{2T+1} + \dots + f_0(\theta)}{z^{2T+2} + g_{2T+1}(\theta)z^{2T+1} + \dots + g_0(\theta)}. \quad (4)$$

III. STRUCTURAL IDENTIFIABILITY USING COEFFICIENT MAPPING

The structural identifiability analysis, by using the coefficient mapping method, is based on the following lemma.

Lemma 1 ([50]): Consider a model structure $\mathcal{M}(\theta)$, where θ represents the parameter vector. Let assume that a transfer function of the model structure is given by (4). Then, the model structure $\mathcal{M}(\theta)$ is

- *globally identifiable* if there is a one-to-one map between the coefficients of the transfer function and the parameter vector θ ,
- *identifiable* if there is a many-to-one map between the coefficient of the transfer function and the parameter vector θ ,
- *unidentifiable* if there is an infinitely many-to-one map between the coefficient of the transfer function and the parameter vector θ . \square

The one-to-one map between the coefficients of the transfer function and the parameter vector θ means that the parameters R_∞ , R_1 , C_1 , α_1 , C_2 , and α_2 are uniquely computed given the coefficients of the transfer function. Likewise, the (infinitely) many-to-one map between the coefficients of the transfer function and the parameter vector θ means that coefficients of the transfer function result in (infinitely) many sets of R_∞ , R_1 , C_1 , α_1 , C_2 , and α_2 .

In order to overcome the computational issue seen in [59], the coefficients with highest indices, i.e., f_{2T+2} , f_{2T+1} , g_{2T+1} , f_{2T} , g_{2T} , etc., are processed in this paper. The denominator coefficients are given by:

$$g_{2T+1}(\theta) = -(a_{1,0} + a_{2,0}) \quad (5)$$

$$g_{2T}(\theta) = -(a_{1,1} + a_{2,1}) + a_{1,0}a_{2,0} \quad (6)$$

$$g_{2T-1}(\theta) = -(a_{1,2} + a_{2,2}) + a_{1,0}a_{2,1} + a_{1,1}a_{2,0} \quad (7)$$

From (3),

$$a_{2,0} = \alpha_2 \quad (8)$$

By using (5) and (8), it is deduced that:

$$a_{1,0} = -(g_{2T+1} + \alpha_2) \quad (9)$$

From Lemma 3 in [59], the relationship between $a_{i,j}$ and $a_{i,j+1}$ is given by:

$$a_{i,j+1} = -\frac{\alpha_i - j - 1}{j + 2} a_{i,j} \text{ for } j \geq 1 \quad (10)$$

By using (8), (9), and (10), the manipulation of g_{2T} and g_{2T-1} results in:

$$a_{1,1} = \frac{B}{C} \quad (11)$$

$$a_{2,1} = A - \frac{B}{C} \quad (12)$$

where,

$$B = g_{2T-1} - (\alpha_2(g_{2T+1} + \alpha_2) + g_{2T})(g_{2T+1} + \frac{2\alpha_2 + 2}{3})$$

$$C = g_{2T+1} + \frac{\alpha_1 + 5\alpha_2}{3} \quad (13)$$

$$A = -(\alpha_2(g_{2T+1} + \alpha_2) + g_{2T}) \quad (14)$$

Thus, $a_{1,0}$, $a_{2,0}$, $a_{1,1}$, and $a_{2,1}$ are written in terms of α_1 and α_2 . From the coefficients of the numerator, it is deduced that:

$$f_{2T+1} - dg_{2T+1} = b_1 + b_2 \quad (15)$$

$$f_{2T} - dg_{2T} = -b_1a_{2,0} - b_2a_{1,0} \quad (16)$$

The solutions of (15) and (16) are given by:

$$b_1 = \frac{D}{E}, \text{ and} \quad (17)$$

$$b_2 = (f_{2T+1} - dg_{2T+1}) - b_1 \quad (18)$$

where,

$$D = (f_{2T+1} - dg_{2T+1})(g_{2T+1} + \alpha_2) - (f_{2T} - dg_{2T})$$

$$E = g_{2T+1} + 2\alpha_2$$

For the next two coefficients, i.e., f_{2T-1} and f_{2T-2} , the following equations hold:

$$f_{2T-1} - dg_{2T-1} = -b_1a_{2,1} - b_2a_{1,1} \quad (19)$$

$$f_{2T-2} - dg_{2T-2} = -b_1a_{2,2} - b_2a_{1,2} \quad (20)$$

The replacement of b_1 , b_2 , $a_{1,0}$, $a_{2,0}$, $a_{1,1}$ and $a_{2,1}$ in (19) and (20) yields:

$$(f_{2T+1} - dg_{2T+1})BE + (f_{2T-1} - dg_{2T-1})CE + ACD - 2BD = 0 \quad (21)$$

$$(f_{2T+1} - dg_{2T+1})(\alpha_1 - 1)BE + (\alpha_2 - 2)ADC - (\alpha_1 + \alpha_2 - 4)BD - 3(f_{2T-2} - dg_{2T-2})CE = 0 \quad (22)$$

In (21) and (22), all terms of A , B , D and E are only dependent on α_2 . Thus, α_1 is expressed as a function of α_2 by solving and rearranging (21) and (22), which lead to:

$$\alpha_1 = \frac{K_1^4(\alpha_2)}{K_2^3(\alpha_2)} = \frac{K_3^5(\alpha_2)}{K_4^4(\alpha_2)} \quad (23)$$

where K_i^j represents the i th polynomial with degree of j .

The exponent α_2 is found by solving the following equation.

$$\frac{K_1^4(\alpha_2)}{K_2^3(\alpha_2)} - \frac{K_3^5(\alpha_2)}{K_4^4(\alpha_2)} = 0 \quad (24)$$

Since the resulting equation is of order eight, it is only possible to solve it numerically. If there is at least one set of $\alpha_i \in (0, 1)$, $i = 1, 2$, then the model is identifiable. After obtaining $\alpha_i \in (0, 1)$, $i = 1, 2$, other parameters are found by calculating $a_{1,0}$, b_1 and b_2 and equations in (3).

TABLE I: transfer function coefficient

Num. Coef.	Value	Den. Coef.	Value
f_{2T+2}	0.01	g_{2T+1}	-1.2962
f_{2T+1}	-0.0121	g_{2T}	0.1931
f_{2T}	0.0015	g_{2T-1}	0.0450
f_{2T-1}	3.505×10^{-4}	g_{2T-2}	0.0191
f_{2T-2}	1.416×10^{-4}	g_{2T-3}	0.0103
f_{2T-3}	7.218×10^{-5}	g_{2T-4}	0.0063

TABLE II: Real Solutions for α_1 and α_2

Roots	α_2	α_1
pair 1	0.298245954619025	2.397337600606689
pair 2	0.500000000000000	0.800000000000000
pair 3	0.625975537273579	0.677356198694181
pair 4	0.646678864697306	0.655173050215288
pair 5	0.797894050107465	0.499243173767398
pair 6	1.295547992101849	-2.589172586806396

The parameters b_1 and b_2 are positive. The α_2 value between $(f_{2T}-dg_{2T})/(f_{2T+1}-dg_{2T+1})-g_{2T+1}$ and $-(f_{2T}-dg_{2T})/(f_{2T+1}-dg_{2T+1})$ leads to negative b_1 and b_2 . Thus, acceptable α_2 's meet the following criterion.

$$\alpha_2 \notin \left(\frac{f_{2T}-dg_{2T}}{f_{2T+1}-dg_{2T+1}} - g_{2T+1}, -\frac{f_{2T}-dg_{2T}}{f_{2T+1}-dg_{2T+1}} \right) \quad (25)$$

If more coefficients of the transfer function are considered, equations with higher degrees are achieved. However, their solutions must meet the equation (24). Thus, (24) is the lowest order equation that is required for structural identifiability analysis.

IV. RESULTS

The proposed structural identifiability analysis method is applied to a battery cell FO-ECM in Fig. 1 with $\alpha_1 = 0.8$, $\alpha_2 = 0.5$, $R_\infty = 0.01$, $R_1 = 0.2$, $C_1 = 3$, and $C_2 = 400$. These values are within the range commonly used in literature, [22]. By using the equations in (3), the coefficients of the original transfer function are computed and given in Table I. The question is that whether it is possible to compute α_1 , α_2 , R_∞ , R_1 , C_1 , and C_2 , given the coefficients of the original transfer function? It is recalled that structural identifiability is a noise-free concept.

In order to increase the accuracy of computations, the Matlab command 'vpa(x,digits)' is used, where 'digits' denotes the digit accuracy.

At the first step, solutions of the exponent α_2 are computed by solving the following equation that is obtained from (24):

$$\begin{aligned} \alpha_2^8 &- 5.395708923047713\alpha_2^7 \\ &+ 12.451808248913298\alpha_2^6 - 16.088049799882121\alpha_2^5 \\ &+ 12.743527275051907\alpha_2^4 - 6.338984994985100\alpha_2^3 \\ &+ 1.932660443044634\alpha_2^2 - 0.329710967652997\alpha_2 \\ &+ 0.024032821066090 = 0 \end{aligned}$$

Two complex roots are obtained, which are not acceptable. The real roots are listed in Table II.

Among the pairs listed in Table II, four pairs are located in interval (0, 1), which are acceptable. From (25), α_2 in range

of (0.52024,0.77595) leads to non-positive value for b_1 and b_2 , and can thus be removed. Only two pairs, pair2 and pair5 in Table II, are left at this stage. The analysis is continued by comparing the transfer function built from the remaining two pairs and the original transfer function. Table III shows the normalized errors between the coefficients of the estimated and original transfer functions, Δg_i , for both pair2 and pair5, where i denotes the index of the coefficient. It is seen that the solution pair2 is only acceptable, because of negligible error achieved. Only one answer was then found for both α_1 and α_2 , thus the model is globally structurally identifiable. Other system parameters are easily calculated after that α_1 and α_2 are found.

Structural identifiability of the FO-ECM in Fig. 1 is then tested for various parameter sets chosen in the range of $R_\infty \in (0.01, 0.2)$, $R_1 \in (0.05, 5)$, $C_1 \in (1, 20)$, $C_2 \in (100, 500)$, $\alpha_1 \in (0.1, 0.9)$, $\alpha_2 \in (0.1, 0.9)$. These ranges are commonly used in battery literature, [22]. It is observed that in all cases, there is a one-to-one map, which demonstrates the global identifiability of the EIS models in these ranges. Fig. 2 shows the impedance spectra of undertaken models.

V. CONCLUSIONS AND FUTURE WORKS

In this paper, an efficient method was proposed for numerical structural identifiability analysis of fractional-order equivalent circuit models (FO-ECMs) with two constant phase elements (CPEs) under the Grünwald-Letnikov differentiation, obtained through impedance spectroscopy. The proposed method confirms that the two-CPE FO-ECM in Fig. 1 is globally identifiable for a wide range of parameter values that is common in battery applications. Structural identifiability analysis for higher-order FO-ECMs and/or by using other approximations of fractional derivatives, as well as practical identifiability analysis, i.e., selection of the excitation signal, the effect of measurement noise, etc., are suggested for future research.

REFERENCES

- [1] J. D. Weiland, D. J. Anderson, "Chronic neural stimulation with thin-film, iridium oxide electrodes," *IEEE Trans. on Biomedical Engineering*, 47(7), pp. 911-918, 2000.
- [2] S. F. Lempka, S. Miocinovic, M. D. Johnson, J. L. Vitek, C. C. McIntyre, "In vivo impedance spectroscopy of deep brain stimulation electrodes," *Journal of Neural Engineering*, 6(4): 046001, 2009.
- [3] C. Jiang, L. Li, H. Hao, "Carbon Nanotube Yarns for Deep Brain Stimulation Electrode," *IEEE Trans. on Neural Systems and Rehabilitation Engineering*, 19(6), pp. 612-616, 2011.
- [4] A. Mercanzini, P. Colin, J.-C. Bensadoun, A. Bertsch, P. Renaud, "In Vivo Electrical Impedance Spectroscopy of Tissue Reaction to Microelectrode Arrays," *IEEE Trans. on Biomedical Engineering*, 56(7), pp. 1909-1918, 2009.
- [5] S. Venkatraman, J. Hendricks, Z. A. King, A. J. Sereno, S. Richardson-Burns, D. Martin, J. M. Carmena, "In Vitro and In Vivo Evaluation of PEDOT Microelectrodes for Neural Stimulation and Recording," *IEEE Trans. on Neural Systems and Rehabilitation Engineering*, 19(3), pp. 307-316, 2011.
- [6] G. Besancon, G. Becq, A. Voda, "Fractional-Order Modeling and Identification for a Phantom EEG System," *IEEE Trans. Control Systems Technology*, 21(1), pp. 130-138, 2020.
- [7] R. J. Halter, A. Hartov, J. A. Heaney, K. D. Paulsen, A. R. Schned, "Electrical Impedance Spectroscopy of the Human Prostate," *IEEE Trans. Biomedical Engineering*, 54(7), pp. 1321-1327, 2007.

TABLE III: Normalized errors between the coefficients of the estimated and original transfer functions, for both pair2 and pair5.

	Δg_{2T}	Δg_{2T-1}	Δg_{2T-2}	Δg_{2T-3}	Δg_{2T-4}	Δg_{2T-5}	$\max\{\Delta g_i\}$ for $i = 1 : 15$
pair 2	$4.7559e^{-40}$	$1.01986e^{-39}$	$1.20208e^{-39}$	$2.23045e^{-40}$	$9.06007e^{-40}$	$3.42014e^{-40}$	$2.63764e^{-39}$
pair 5	0.00598	0.00112	0.00779	0.01049	0.012981	0.030246	0.03169

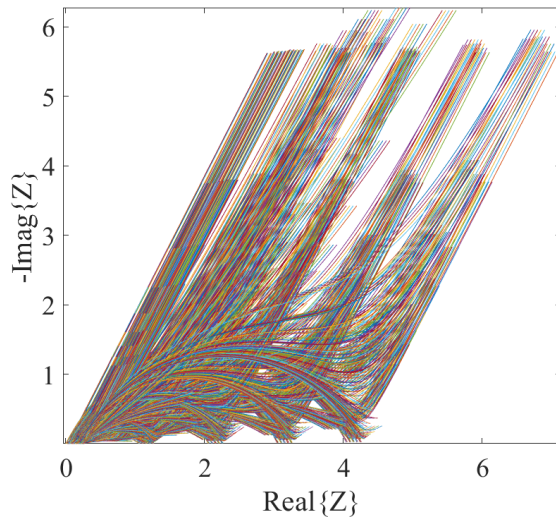


Fig. 2: The proposed method confirms that the FO ECM with two CPEs and Grünwald-Letnikov differentiation is globally structurally identifiable for batteries with the shown impedance spectra.

- [8] V. Mishra, H. Bouayad, A. Schned, A. Hartov, J. Heaney, and R. J. Halter, "A Real-Time Electrical Impedance Sensing Biopsy Needle," *IEEE Trans. on Biomedical Engineering*, 59(12), pp. 3327–3336, 2012.
- [9] Z. Haeri, M. Shokoufi, M. Jenab, R. Janzen, F. Golnaraghi, "Electrical impedance spectroscopy for breast cancer diagnosis: Clinical study," *Integrative Cancer Science and Therapeutics*, 3(6), pp. 1–6, 2016.
- [10] R. P. Braun, J. Mangana, S. Goldinger, L. French, R. Dummer, A. A. Marghoob, "Electrical Impedance Spectroscopy in Skin Cancer Diagnosis," *Dermatologic Clinics*, 35(4), pp. 489–493, 2017.
- [11] T. E. Kerner, K. D. Paulsen, A. Hartov, S. K. Soho, S. P. Poplack, "Electrical impedance spectroscopy of the breast: clinical imaging results in 26 subjects," *IEEE Trans. on Medical Imaging*, 21(6), pp. 638–645, 2002.
- [12] T.-J. Kao, G. Boverman, B. S. Kim, D. Isaacson, G. J. Saulnier, J. C. Newell, M. H. Choi, R. H. Moore, and D. B. Kopans, "Regional Admittivity Spectra With Tomosynthesis Images for Breast Cancer Detection: Preliminary Patient Study," *IEEE Trans. Medical Imaging*, 27(12), pp. 1762–1768, 2008.
- [13] R. Wang, J. Di, J. Ma, Z. Ma, "Highly sensitive detection of cancer cells by electrochemical impedance spectroscopy," *Electrochimica Acta*, 61, pp. 179–184, 2012.
- [14] L. Han, P. Liu, V. A. Petrenko, A. Liu, "A Label-Free Electrochemical Impedance Cytosensor Based on Specific Peptide-Fused Phage Selected from Landscape Phage Library," *Scientific Reports*, 6, Article number: 22199, 2016.
- [15] R. R. Sevag-Packard, Y. Luo, P. Abiri, N. Jen, O. Aksoy, W. M. Suh, Y.-C. Tai, T. K. Hsiai, "3-D Electrochemical Impedance Spectroscopy Mapping of Arteries to Detect Metabolically Active but Angiographically Invisible Atherosclerotic Lesions," *Theranostics*, 7(9), pp. 2431–2442, 2017.
- [16] F. Zhang, T. Jin, Q. Hu, P. He, "Distinguishing skin cancer cells and normal cells using electrical impedance spectroscopy," *Journal of Electroanalytical Chemistry*, 823, pp. 531–536, 2018.
- [17] R. Salahandish, A. Ghaffarinejad, S. M. Naghib, K. Majidzadeh-A, H. Zargartalebi, A. Sanati-Nezhad, "Nano-biosensor for highly sensitive detection of HER2 positive breast cancer," *Biosensors and Bioelectronics*, 117, pp. 104–111, 2018.
- [18] E. Barsoukov and J. R. Macdonald, *Impedance spectroscopy: theory, experiment, and applications*, John Wiley & Sons, 2005.
- [19] S. Buller, M. Thele, R. De Doncker, and E. Karden, "Impedance-based simulation models of supercapacitors and li-ion batteries for power electronic applications," *IEEE Trans. Industry Applications*, 41(3), pp. 742–747, 2005.
- [20] U. Tröltzsch, O. Kanoun, and H.-R. Tränkler, "Characterizing aging effects of lithium ion batteries by impedance spectroscopy," *Electrochimica Acta*, 51(8), pp. 1664–1672, 2006.
- [21] A. Guha, A. Patra, "Online Estimation of the Electrochemical Impedance Spectrum and Remaining Useful Life of Lithium-Ion Batteries," *IEEE Trans. on Instrumentation and Measurement*, 67(8), pp. 1836–1849, 2018.
- [22] P. E. Jacob, S. M. M. Alavi, A. Mahdi, S. J. Payne, D. A. Howey, "Bayesian Inference in Non-Markovian State-Space Models With Applications to Battery Fractional-Order Systems," *IEEE Trans. on Control Systems Technology*, 26 (2), pp. 497–506, 2018.
- [23] H. Blanke, O. Bohlen, S. Buller, R. W. De Doncker, B. Fricke, A. Hammouche, D. Linzen, M. Thele, D. U. Sauer, "Impedance measurements on lead-acid batteries for state-of-charge, state-of-health and cranking capability prognosis in electric and hybrid electric vehicles," *Journal of Power Sources*, 144(2), pp. 418–425, 2015.
- [24] R. R. Richardson, P. T. Ireland, and D. A. Howey, "Battery internal temperature estimation by combined impedance and surface temperature measurement," *Journal of Power Sources*, 265, pp. 254–261, 2014.
- [25] C. de Beer, P. S. Barendse, P. Pillay, "Fuel Cell Condition Monitoring Using Optimized Broadband Impedance Spectroscopy," *IEEE Trans. on Industrial Electronics*, 62(8), pp. 5306–5316, 2015.
- [26] J. G. Zhu, Z. C. Sun, X. Z. Wei, H. F. Dai, "A new lithium-ion battery internal temperature on-line estimate method based on electrochemical impedance spectroscopy measurement," *Journal of Power Sources*, Vol. 274, pp. 990–1004, 2015.
- [27] E. Din, C. Schaefer, K. Moffat, J. T. Stauth, "A Scalable Active Battery Management System With Embedded Real-Time Electrochemical Impedance Spectroscopy," *IEEE Trans. on Power Electronics*, 32(7), pp. 5688–5698, 2017.
- [28] D. A. Howey, P. D. Mitcheson, V. Yufit, G. J. Offer, N. P. Brandon, "On-line measurement of battery impedance using motor controller excitation," *IEEE Trans. on Vehicular Technology*, 63(6), pp. 2557–2566, 2014.
- [29] S. M. M. Alavi, C. R. Birkl, and D. A. Howey, "Time-domain fitting of battery electrochemical impedance models," *Journal of Power Sources*, 288, pp. 345–352, 2015.
- [30] J. Tian, R. Xiong, Q. Yu, "Fractional-Order Model-Based Incremental Capacity Analysis for Degradation State Recognition of Lithium-Ion Batteries," *IEEE Trans. on Industrial Electronics*, 66(2), pp. 1576–1584, 2019.
- [31] Y. Ma, X. Zhou, B. Li, and H. Chen, "Fractional Modeling and SOC Estimation of Lithium-ion Battery," *IEEE/CAA Journal of Automatica Sinica*, 3(3), pp. 281–287, 2016.
- [32] R. Xiong, J. Tian, W. Shen, F. Sun, "A novel fractional order model for state of charge estimation in lithium ion batteries," *IEEE Trans. on Vehicular Technology*, 68(5), pp. 4130–4139, 2019.
- [33] J. Sabatier, J. M. Francisco, F. Guillemand, L. Lavigne, M. Moze, and M. Merveillaut, "Lithium-ion batteries modeling: A simple fractional differentiation based model and its associated parameters estimation method," *Signal Processing*, 107, pp. 290–301, 2015.
- [34] E. Sadeghi, M. H. Zand, M. Hamzeh, M. Saif, S. M. M. Alavi, "Controllable Electrochemical Impedance Spectroscopy: From Circuit Design to Control and Data Analysis," *IEEE Trans. on Power Electronics*, 35(9), pp. 9935–9944, 2020.
- [35] S. M. M. Alavi, A. Mahdi, S. J. Payne, D. A. Howey, "Identifiability of generalised Randles circuit models," *IEEE Trans. on Control Systems Technology*, 25(6), 2112–2120, 2017.
- [36] C. Zou, L. Zhang, X. Hu, Z. Wang, T. Wik, M. Pecht, "A review of fractional-order techniques applied to lithium-ion batteries, lead-acid

- batteries, and supercapacitors,” *Journal of Power Sources*, 390, pp. 286–296, 2018.
- [37] J. P. Tian, R. Xiong, W. X. Shen, F. C. Sun, “Fractional order battery modelling methodologies for electric vehicle applications: Recent advances and perspectives,” *Science China Technological Sciences*, 63, pp. 2211–2230, 2020.
- [38] Y. N. Wang, Y. Q. Chen, X. Z. Liao, “State-of-art survey of fractional order modeling and estimation methods for lithium-ion batteries,” *Fractional Calculus and Analysis*, 22(6), pp. 1449–1479, 2019.
- [39] Q. Yang, J. Xu, B. Cao, X. Li, “A simplified fractional order impedance model and parameter identification method for lithium-ion batteries,” *PLoS ONE*, 12(2), e0172424, 2017.
- [40] D. J. Bates, J. D. Hauenstein, N. Meshkat, “Identifiability and numerical algebraic geometry,” *PLoS ONE*, 14(12), e0226299, 2019.
- [41] L. Ljung, “System identification: theory for the user,” *PTR Prentice Hall Information and System Sciences Series*, vol. 198, 1987.
- [42] T. Soderstrom and P. Stoica, “*System identification*,” Prentice hall London, 1989.
- [43] A. Sharma and H. K. Fathy, “Fisher identifiability analysis for a periodically-excited equivalent-circuit lithium-ion battery model,” in *American Control Conference (ACC)*, pp. 274–280, 2014.
- [44] M. J. Rothenberger, J. Anstrom, S. Brennan, and H. K. Fathy, “Maximizing parameter identifiability of an equivalent-circuit battery model using optimal periodic input shaping,” in *ASME 2014 Dynamic Systems and Control Conference*, 2014.
- [45] H. Pohjanpalo, “System identifiability based on the power series expansion of the solution,” *Mathematical biosciences*, 41(1), pp. 21–33, 1978.
- [46] M. J. Chappell, K. R. Godfrey, and S. Vajda, “Global identifiability of the parameters of nonlinear systems with specified inputs: a comparison of methods,” *Mathematical Biosciences*, 102(1), pp. 41–73, 1990.
- [47] S. Vajda, K. R. Godfrey, and H. Rabitz, “Similarity transformation approach to identifiability analysis of nonlinear compartmental models,” *Mathematical biosciences*, 93(2), pp. 217–248, 1989.
- [48] F. Anstett, G. Bloch, G. Millérioux, and L. Denis-Vidal, “Identifiability of discrete-time nonlinear systems: The local state isomorphism approach,” *Automatica*, 44(11), pp. 2884–2889, 2008.
- [49] N. Meshkat and S. Sullivant, “Identifiable reparametrizations of linear compartment models,” *Journal of Symbolic Computation*, 63, pp. 46–67, 2014.
- [50] A. Mahdi, N. Meshkat, and S. Sullivant, “Structural identifiability of viscoelastic mechanical systems,” *PloS one*, 9(2), p. e86411, 2014.
- [51] K. Glover and J. C. Willems, “Parametrizations of linear dynamical systems: canonical forms and identifiability,” *IEEE Trans. on Automatic Control*, 19(6), pp. 640–646, 1974.
- [52] J. Distefano III, “On the relationships between structural identifiability and the controllability, observability properties,” *IEEE Trans. on Automatic Control*, 22(4), pp. 652–652, 1977.
- [53] J. Van den Hof, “Structural identifiability of linear compartmental systems,” *IEEE Trans. on Automatic Control*, 43(6), pp. 800–818, 1998.
- [54] L. Ljung and T. Glad, “On global identifiability for arbitrary model parametrizations,” *Automatica*, 30(2), pp. 265–276, 1994.
- [55] S. Audoly, G. Bellu, L. D’Angio, M. P. Saccomani, and C. Cobelli, “Global identifiability of nonlinear models of biological systems,” *IEEE Trans. on Biomedical Engineering*, 48(1), pp. 55–65, 2001.
- [56] C. Cobelli and J. DiStefano, “Parameter and structural identifiability concepts and ambiguities: a critical review and analysis,” *American Journal of Physiology- Regulatory, Integrative and Comparative Physiology*, 239(1), pp. R7–R24, 1980.
- [57] R. Bellman and K. J. Åström, “On structural identifiability,” *Mathematical biosciences*, 7(3), pp. 329–339, 1970.
- [58] P. Nazarian, M. Haeri, and M. S. Tavazoei, “Identifiability of fractional order systems using input output frequency contents,” *ISA transactions*, 49(2), pp. 207–214, 2010.
- [59] S. M. M. Alavi, A. Mahdi, P. E. Jacob, S. J. Payne, D. A. Howey, “Structural Identifiability Analysis of Fractional Order Models with Applications in Battery Systems,” *arXiv:1511.01402*, 2015.